

Design and Fabrication of a 315 μH Bondwire Micro-Transformer for Ultra-Low Voltage Energy Harvesting

Enrico Macrelli^{*}, Ningning Wang[†], Saibal Roy[†], Michael Hayes[†], Rudi Paolo Paganelli[‡], Marco Tartagni^{*}, and Aldo Romani^{*}

^{*}University of Bologna (DEI), Bologna, Italy

[†]Tyndall National Institute, University College Cork, Ireland

[‡]National Research Council (CNR-IEIT), Bologna, Italy

Abstract—This paper presents a design study of a new topology for miniaturized bondwire transformers fabricated and assembled with standard IC bonding wires and toroidal ferrite (Fair-Rite 5975000801) as a magnetic core. The micro-transformer realized on a PCB substrate, enables the build of magnetics on-top-of-chip, thus leading to the design of high power density components. Impedance measurements in a frequency range between 100 kHz to 5 MHz, show that the secondary self-inductance is enhanced from 0.3 μH with an epoxy core to 315 μH with the ferrite core. Moreover, the micro-machined ferrite improves the coupling coefficient from 0.1 to 0.9 and increases the effective turns ratio from 0.5 to 35. Finally, a low-voltage IC DC-DC converter solution, with the transformer mounted on-top, is proposed for energy harvesting applications.

Keywords—bonding wires; bondwire; converter; DC-DC; energy harvesting; ferrite; magnetics; on-chip; PCB; transformer.

I. INTRODUCTION

Recently many efforts have been devoted to the miniaturization of energy harvesting (EH) circuits and transducers. However, the development of micro-magnetic components is required as well. The main limitation to achieve high frequency and high current in DC-DC converters is the design of power inductors and transformers [1] [2]. Overall size reduction of power converters is a key technology, requiring the minimization of power losses as well. The ultimate market evolution is the growth of new miniaturized platforms, which can be referred to as power supply in package (PwrSiP) and power supply on chip (PwrSoC) [1]. In PwrSiP magnetics are co-packaged with the IC active circuitry, while in PwrSoC the magnetics are integrated, which potentially lead to the realization of the ‘holy grail’ of fully integrated power supplies. In general, on-chip magnetics require costly and complex deposition techniques, which limit their application when magnetics are not in mass production through commercial foundries. Current research is focused on integrated magnetics by using microelectromechanical system (MEMS) technology. Due to the process constraints, the resulting MEMS inductors and transformers have a limited efficiency [3].

Wire bonding is commonly used in all modern power management integrated circuit (IC) packages [4]. All bonding

processes are based on solid phase welding, where two materials are brought into contact by means of pressure. Bonding wires act as a natural inductor, however the inductance value of a single wire is inadequate for power converters. Bondwire magnetics is a simple approach to fabricate magnetics by using standard bonding wires, which can be easily integrated into the IC packaging processes [3].

In this paper we present a new cost-effective approach to realize bondwire transformers by using gold bonding wires and micro-machined soft ferrite core. It will be shown how this technique is suitable for incorporation of magnetics on-top of an IC, thus making possible the design of high power density components with a wafer level integration.

II. BASIC RELATIONSHIPS

The device presented in this paper is a two-winding transformer, with bonding wires as coils completed on the metallization layer, and a toroidal ferrite as a magnetic core. The low-frequency self-inductance of each winding L (H) is estimated by the reluctance formula as [5]:

$$L = \frac{\mu_0 \mu_{rc} n^2 A_c}{l_c} \quad (1)$$

where $\mu_0 = 4 \cdot \pi \cdot 10^{-7}$ H/m is the free-space permeability, μ_{rc} is the core relative permeability, A_c (m^2) is the cross-sectional area of the core, l_c (m) is the mean magnetic path length, and n is the number of turns of the coil considered. The low-frequency series resistance of the winding R (Ω) can be expressed as $R = n \cdot (R_b + R_m)$, where R_b (Ω) is the bonding wire resistance, and R_m (Ω) is the printed circuit board (PCB) metal conductor resistance [5] [6]. Since in a real transformer not all flux produced by the primary winding is coupled to the secondary one, the mutual inductance L_{12} (H) is defined by:

$$L_{12} = k \sqrt{L_{11} \cdot L_{22}} \quad (2)$$

where k is the coupling coefficient which measures the magnetic coupling between the coils, and L_{11} (H) and L_{22} (H) are the self-inductances evaluated by (1) of primary and

This research was partially funded by the European Community's FP7 2007-2013 under grant agreement Nanofunction no. 257375 and by the ENIAC-JTI under grant agreement LAB4MEMs no. 325622.

secondary windings, respectively. For the transformer we can define the turns ratio $n_{12} = n_2/n_1 = (L_{22}/L_{11})^{1/2}$ where n_1 and n_2 are the number of turns of each side. The coupling coefficient k has to be taken into account in n_{12} , thus getting the effective turns ratio $n_e = k \cdot n_{12}$.

The minimum frequency f_{\min} (Hz) at which the primary winding can operate without saturating the core, is estimated by applying a sinusoidal waveform voltage as follows:

$$f_{\min} = \frac{V_{\max}}{2\pi n_1 A_c B_s} \quad (3)$$

where V_{\max} (V) is the peak amplitude of the sinusoidal voltage, and B_s (T) is the saturation magnetic flux density. At high frequencies the current density becomes non uniform due to eddy currents which cause skin effect. Hence, the transformer behavior can be considered in the low-frequency region only if the core skin depth is much greater than the core thickness.

The power loss of the device P_C (mW) is calculated by evaluating the power dissipation in the core due to eddy currents and hysteresis losses [5] [6], and is expressed as:

$$P_C = k_c f_{op}^a (10^4 B_m)^b V_c \quad (4)$$

where f_{op} (kHz) is the operating frequency, B_m (T) is the amplitude of the AC component of the magnetic flux density, $V_c = A_c \cdot l_c$ (cm³) is the core volume, and k_c , a , and b are constants for the core material.

III. DESIGN AND FABRICATION

Different prototypes are designed and fabricated on a single layer PCB substrate (370HR material) with ultra-thin and ultra-narrow technology (0.33 mm thick), copper conductor ($t_m = 15 \mu\text{m}$, $\rho_m = 1.68 \cdot 10^{-6} \Omega\text{-cm}$) plus a nichel-gold finish by Litho-Circuits. A Kulicke & Soffa (K&S) 4524 gold wire bonder was used to assembly the devices.

Key design parameters in terms of bonding wires include wire diameter, material, and minimum spacing. Gold round bonding wires are used due to the low resistivity of gold ($\rho_b = 2.44 \cdot 10^{-6} \Omega\text{-cm}$) which minimizes the wire series resistance, while a small spacing between wires enhances the self-inductance and the coupling coefficient of the device. Several tests are performed with two different gold wire diameters d_b (m), minimum bond pad pitch BPP_{\min} (m), and ball spread on blank silicon substrate. The tests show that thick round wires ($d_b = 32 \mu\text{m}$) have the advantages of being robust enough to touch the core without breaking, while the large diameter leads to small series resistance. However, thin round wires ($d_b = 25 \mu\text{m}$) allow to bond with higher BPP_{\min} , while they are more brittle and lead to high series resistance. We chose thick round wires as the best choice for our design.

With the aim to evaluate the bonding capability and maximize the number of turns with fixed footprint area of $A_f = 4.95 \text{ mm} \times 4.95 \text{ mm}$, several layouts are designed depending on the PCB technology parameters such as

conductor width w_m (m) and minimum spacing s_{\min} (m), and wire bonder constraints such as BPP_{\min} and outer-inner pad distances $d_{\text{ext}} - d_{\text{int}}$ (m) from magnetic core. The first layout T_1 is designed with the smallest conductors thus allowing a higher turns ratio device. The second layout T_2 is designed with the larger and wider conductors which allows better performance in wire bonding. The third layout T_3 is designed with the highest inner pad distance from core thus permitting the mounting of thick cores, however this reduces the turns number. The last layout T_4 has the same specifics of T_1 , yet it has two turns of primary winding. The bondwire transformer layouts are shown in Table I.

In order to increase the inductance and improve the coupling coefficient of the devices, a soft ferrite core is employed as a magnetic core. The ferrite is the commercial Fair-Rite 5975000801, which is a Mn-Zn uncoated toroidal soft ferrite with resistivity $\rho_c = 3 \Omega\text{-m}$, relative permeability $\mu_{rc} = 5000$, coercivity $H_c = 13 \text{ A/m}$, and saturation flux density $B_s = 0.43 \text{ T}$. The outer and inner diameters are $D_o = 3.95 \text{ mm}$ and $D_i = 2.15 \text{ mm}$, respectively, while the core thickness is $t_c = 1.40 \text{ mm}$. The core loss constants are $k_c = 6.6 \cdot 10^{-8}$, $a = 1.52$, and $b = 2.19$ evaluated at $f_{op} = 100 \text{ kHz}$ and 100°C . Finally, an epoxy air-core with the same dimension is used to compare the performance between magnetic and air-core transformers. The assembly of the ferrite involves two micro-machining steps represented by thinning and coating. In the first step the core thickness is reduced to about $t_c \cong 0.5 \text{ mm}$ with a polishing machine, which represents the minimum height for getting a good yield in wire bonding. In the second step the thinned core is coated with an insulation film to prevent any conductive paths. Fig. 1 shows the micro-machining steps of the ferrite core. After the fabrication, the toroidal core is assembled to the PCB substrate, and bonded with a K&S 4524 wire bonder from inner to outer pads. Fig. 2 shows a microphotograph of the T_1 bondwire transformer assembled with 5975000801 toroidal ferrite core and gold round bonding wires. The prototype is realized with the wire bonder in manual mode with the work-holder temperature fixed at 100°C .

In order to design properly the device, the analytical performance of the micro-transformers are evaluated. The DC secondary self-inductance L_{22} is evaluated by (1), and the DC secondary series resistance R_{22} (Ω) is estimated. The inductance analysis of the bondwire transformer prototypes with the toroidal cores is shown in Table II. The results show that the self-inductance of the T_1 layout increases from 86 nH with epoxy air-core to 426 μH with ferrite core.

TABLE I. SUMMARY OF THE BONDWIRE TRANSFORMER LAYOUTS

Layout	$n_1 : n_2$	w_m (μm)	s_{\min} (μm)	BPP_{\min} (μm)	$d_{\text{ext}} - d_{\text{int}}$ (μm)
T_1	1:38	80	50	130	450-225
T_2	1:33	90	60	150	450-225
T_3	1:28	90	70	160	450-300
T_4	2:35	80	50	130	450-225

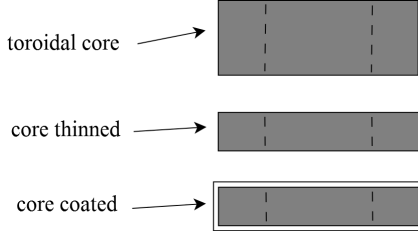


Fig. 1. Micro-fabrication steps of the ferrite core performed during the assembly of the devices.

The minimum frequency f_{\min} without saturating the core is evaluated by (3) on the primary winding, the maximum frequency f_{\max} (Hz) is extracted by evaluating the core skin depth, while the power loss in the core P_C is estimated by (4). The results show that the transformer with 5975000801 core is suitable for applications in the frequency range between $f_{\min} \cong 8.2$ kHz ($V_{\max} = 10$ mV) and $f_{\max} \cong 2.8$ MHz, while the estimated power loss in the core is $P_C \cong 1.16$ mW (at $f_{\text{op}} = 100$ kHz and $B_m = 0.1$ T).

IV. IMPEDANCE MEASUREMENTS

In order to extract the main transformer parameters, open-circuit and short-circuit measurements are performed from the two-port network [5]. Firstly, in an open-circuit test the secondary winding is left open ($I_2 = 0$ A) and an AC voltage with frequency f_{ac} (Hz) is applied to the primary winding. Measurements at the primary terminals give the primary impedance Z_{11} (Ω), hence the primary self-inductance is extracted as $L_{11}' = \text{Im}\{Z_{11}\} / 2 \cdot \pi \cdot f_{\text{ac}}$. In a second open-circuit test, the primary winding is left open ($I_1 = 0$ A) and an AC voltage is applied to the secondary winding. Measurements at the secondary terminals give the secondary impedance Z_{22} (Ω), thus the secondary self-inductance is extracted as $L_{22}' = \text{Im}\{Z_{22}\} / 2 \cdot \pi \cdot f_{\text{ac}}$.

Finally, the mutual inductance L_{12}' (H) is measured with series-aiding and series-opposing measurements. In the series-aiding test the two windings are connected so that the total magnetic flux is equal to the sum of the fluxes in both coils. Measurements at the terminals give the series-aiding inductance $L_a = L_{11}' + L_{22}' + 2 \cdot L_{12}'$ (H). In the series-opposing test the two windings are connected so that the fluxes in the two windings oppose each other. Measurements at the terminals give the series-opposing inductance $L_b = L_{11}' + L_{22}' - 2 \cdot L_{12}'$ (H). Hence, the mutual inductance is extracted as $L_{12}' = (L_a - L_b) / 4$.

TABLE II. RESULTS OF THE INDUCTANCE ANALYSIS OF THE BONDWIRE TRANSFORMERS PROTOTYPES

	Core	T_1	T_2	T_3	T_4
L_{22} (μH) from (1)	5975000801	426	321	231	361
	Dummy epoxy	0.086	0.065	0.047	0.073
R_{22} (Ω)	both	3.8	3.2	2.7	3.5

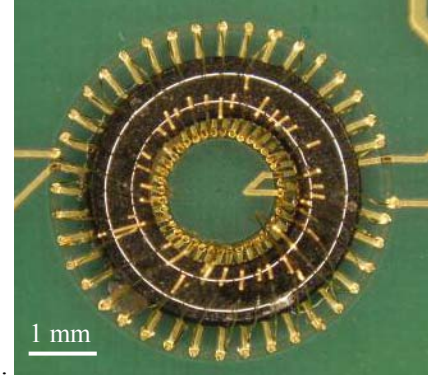


Fig. 2. Microphotograph of the T_1 bondwire transformer assembled with 5975000801 toroidal ferrite core and gold thick bonding wires.

The impedance measurements are performed by using a precision LCR Meter 4285A equipped with a test leads 16048A and a probe station. The LCR Meter is calibrated with an open-circuit and short-circuit tests to compensate the parasitic inductance and reactance of the cables, with an AC voltage level set to 10 mV without bias.

From the impedance measurements of primary, secondary, and mutual inductance, the coupling coefficient k from (2) and the effective turns ratio n_e are extracted. Fig. 3 shows the impedance measurements of the T_1 layout with toroidal ferrite and air-core and thick gold bonding wires. The results for the T_1 layout show that the secondary self-inductance is enhanced from 0.3 μH with epoxy core to 315 μH with 5975000801 core. Furthermore, the ferrite improves the coupling coefficient from 0.1 to 0.9, and increases the effective turns ratio from 0.5 to 35 with respect to the air-core device. Fig. 4 shows the impedance measurements of the secondary self-inductance for all PCB layouts with toroidal ferrite core and thick gold bonding wires. The results show that the secondary self-inductance decreases from 315 μH for the T_1 layout to 180 μH for the T_3 layout, because the less wires number and the higher spacing between wires. Finally, the measured series DC resistances of the T_1 layout are 0.3 Ω and 4.3 Ω for the primary and secondary sides, respectively.

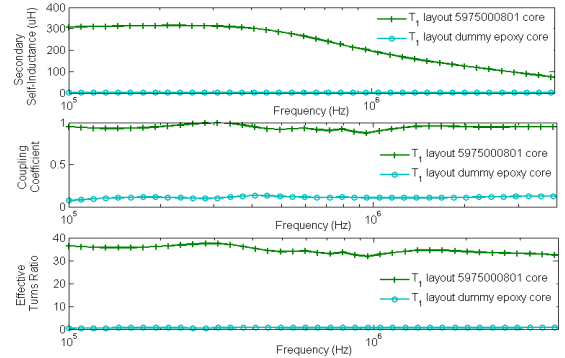


Fig. 3. Measurements of the T_1 transformer layout with toroidal ferrite and epoxy cores: secondary self-inductance (top), coupling coefficient (middle), and effective turns ratio (bottom).

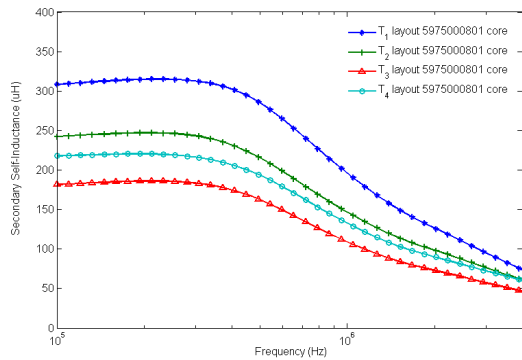


Fig. 4. Measured secondary self-inductance for all PCB layouts with toroidal ferrite core.

V. IC INTEGRATION

Self-startup is one of the most critical issues for battery-less and low input voltage DC-DC converters for EH applications [1]. Standard startup approaches are based on several techniques such as subthreshold charge pumps, mechanical switch, and external voltage. Another approach is based on boost converter with an external transformer. Fig. 5 shows the circuit schematic of a low-voltage converter, based on a Meissner oscillator topology [7] and capable of starting from 30 mV while providing an output voltage higher than 800 mV. The converter is designed in a STMicroelectronics BCD6s 0.32 μm technology and is compatible with the mounting of magnetics on-top of the silicon die. The time-domain simulation response with Cadence Design Systems in Fig. 6 shows that the converter can provide more than 800 mV with an input voltage of 40 mV. The output voltage is higher than the typical threshold voltage of a MOSFET, hence is thus suitable for starting up a more efficient conventional DC-DC converter for steady-state operation. Finally, Fig. 7 shows a microphotograph of the proposed IC converter.

VI. CONCLUSIONS

In this paper we have designed and investigated a cost-effective approach to realize magnetic components by using standard bonding wires and magnetic core. We have fabricated and assembled a new topology for bondwire transformers on a PCB substrate with micro-machined ferrite cores and thick gold bonding wires. In order to maximize the number of turns and to enhance the performance, gold bonding wires are modeled and several layouts are proposed.

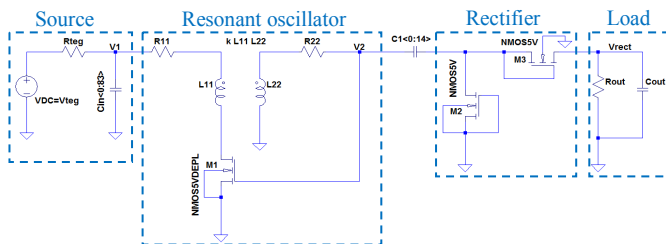


Fig. 5. Circuit schematic of the low-voltage DC-DC converter based on a Meissner oscillator, where the transformer is mounted on-top.

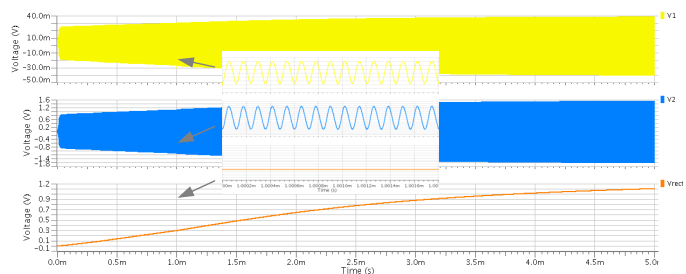


Fig. 6. Time-domain simulation response with Cadence Design Systems of primary voltage (top), secondary voltage (middle), and rectified output voltage (bottom) with an input voltage of 40 mV.

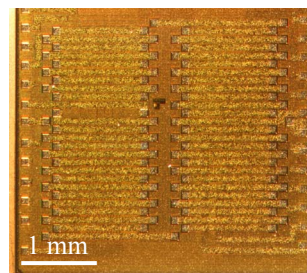


Fig. 7. Microphotograph of the DC-DC converter designed in STM BCD6s 0.32 μm compatible for the assembly of the bondwire magnetics on-top.

Besides, a ferrite core is micro-fabricated to adapt thickness and to allow insulation. Impedance measurements show the achievement of high turn and high inductance devices. Finally, an IC low-voltage DC-DC converter with the magnetics mounted on-top is proposed for EH circuits.

ACKNOWLEDGMENT

The authors thank Mr. Finbarr Waldron and Mr. Kenneth Rodgers of Tyndall National Institute.

REFERENCES

- [1] C. O. Mathúna, N. Wang, S. Kulkarni, and S. Roy, "Review of integrated magnetics for power supply on chip (PwrSoC)," *IEEE Trans. Power Electron.*, vol. 27, no. 11, pp. 4799-4816, Nov. 2012.
- [2] L. Qiang et al., "Technology road map for high frequency integrated DC-DC converter," in *Proc. IEEE Appl. Power Electron. Conf.*, pp. 533-539, 2010.
- [3] J. Lu et al., "Modelling, design and characterization of multiturn bondwire inductors with ferrite epoxy glob cores for power supply system-on-chip or system-in-package applications," *IEEE Trans. Power Electron.*, vol. 25, no. 8, pp. 2010-2017, Aug. 2010.
- [4] G. G. Harman, "Wirebonding in microelectronics", 3 ed. *McGraw-Hill Professional*, 2010.
- [5] M. K. Kazimierczuk, "High-frequency magnetic components", *John Wiley & Sons*, 2009.
- [6] D. Flynn, R. S. Dhariwal, and M. P. Y. Desmulliez, "A design study of microscale magnetic components for operation in the MHz frequency range," *J. Micromech. Microeng.*, vol. 16, pp. 1811-1818, 2006.
- [7] J. M. Damaschke, "Design of a low-input-voltage converter for thermoelectric generator," *IEEE Trans. Ind. Appl.*, vol. 33, no. 5, pp. 1203-1207, Sep./Oct. 1997.